Materials Research. 2022; 25:e20210522
DOI: https://doi.org/10.1590/1980-5373-MR-2021-0522

The Influence of the Molecular Architecture of the Peg: Ppg Triblock Copolymer on the Properties of Epoxy Nanocomposites

Bruna L. Silva[a]*, Marcia B. Schuster[a], Daniela Becker[a], Luiz A.F. Coelho[a]

[a]Universidade do Estado de Santa Catarina - UDESC, Joinville, SC, Brasil.

Received: October 07, 2021; Revised: February 04, 2022; Accepted: March 11, 2022.

This work focuses on characterizing the role of different triblock copolymers on the dispersion of nanoparticles in an epoxy matrix and in the thermal and mechanical properties of the resulting nanocomposites, using Poly (ethylene glycol) - block-poly (propylene glycol) - block-poly (ethylene glycol) (PEG-b-PPG- b-PEG) with 30% PEG, and poly (propylene glycol) - block-poly (ethylene glycol) - block-poly (propylene glycol) (PPG-b-PEG-b-PPG) with 50% PEG. The nanoparticles employed have different geometries: carbon nanotubes, graphene nanoplatelets and carbon black (spherical). Both copolymers were miscible in epoxy. The results suggest that the copolymers viscosity may be interfering with the dispersion of the nanoparticles in the matrix: the PPG-b- PEG-b-PPG50% copolymer has a higher viscosity than the PEG b-PPG-b-PEG30%, which facilitates their dispersion and an increase in mechanical properties. The PEG fraction was an important factor in the dispersion of nanoparticles in the epoxy matrix. The higher the PEG content in the copolymer block, the greater the synergy shown in the mechanical properties, since the nanoparticles inhibited the plasticizing effect of the block copolymer.

Keywords: *Block copolymer, nanocomposites, dispersion, nanoparticles, epoxy.*

1. Introduction

Among the thermoset polymers, epoxy is one of the most used in research and industrial applications, due to its mechanical and thermal properties, and its chemical and dimensional stability. However, due to its network structure, it is a fragile material. Thermosets modified with block copolymers allow improving mechanical properties (such as fracture toughness), due to their ability to self-assemble and form varied morphologies. The most investigated copolymers for epoxy toughening would be those with PEG/PPG blocks, Poly (ethylene glycol)/Poly (propylene glycol) can be found[1-4]. The PEG block is mainly responsible for physical interactions with the aromatic amine epoxy-reticulate. Thus, the final morphology is governed by several factors such as mass/volumetric fraction, block interactions, block size, cure kinetics and diffusion processes[5].

Works such as Larrañaga et al.[6] and Silva et al.[3], which studied epoxy/triblock copolymer systems, showed that the fraction of blocks in the copolymer determines the system's miscibility/immiscibility. That is, regardless of the PEG position, if there is sufficient fraction for the PPG to form the nucleus and the PEG stay at the ends, immiscibility occurs with the epoxy phase, as shown schematically in Figure 1. Although phase separation was observed by those authors, some previous studies showed that the DGEBA/DDM (bisphenol A diglycidyl ether/ 4,4 Diaminodiphenylmethanes) system modified with PEG block copolymers remains miscible due to interactions between the copolymer's ether group and the DGEBA hydroxyl[7-13].

A recent literature review[14] suggests that incorporating nanoparticles with the block copolymer may improve the mechanical and thermal properties of the matrix. The addition of nanoparticles to epoxy/copolymer systems can contribute in a multifunctional way to a polymeric matrix. Block copolymers allow a better dispersion/adhesion of nanoparticles in the thermoset matrix, just like nanoparticles can inhibit the plasticization effect of the block copolymer.

Jayan et al.[15] explored the synergistic effect of adding graphene oxide (GO) and a 5800 g/mol PEG-b-PPG-b-PEG epoxy triblock copolymer and proved that the copolymer was successfully grafted onto the surface of the OG. The arrangement of the graft in the form of a micelle is confirmed through microscopy and resulted in 400% increase in toughness, 100% in Young's modulus and 33% in tensile strength. Kulkarni et al.[16] used the PEO-PPO-PEO triblock copolymer as a surfactant to disperse hexagonal boron nitride (hBN) nanoparticles in an epoxy matrix, observing that the random dispersion of the copolymer-modified hBN nanoparticles in the matrix creates a mechanical interlock, therefore improving their mechanical properties. Gao et al.[17] used PHMA-b-PGMA grafted SiO_2 nanoparticles to toughen an epoxy resin. They observed that adding the hard particles to the copolymer is a promising method to toughen hard polymers. These nanoparticles can also improve the Young's modulus while maintaining the tensile strength, a combination that cannot be achieved just by inserting a rubber copolymer. Although there are several attempts in the literature to increase epoxy resistance using block copolymers, none of them report how the architecture/organization of the blocks

*e-mail: bruna-louise@hotmail.com

influences the nanoparticle dispersion and the properties of the nanocomposites.

Within this context, the present work aims to describe the role of triblock copolymers with different PEG: PPG ratios and positions in epoxy matrix nanocomposites, evaluating their thermal and mechanical properties, the role of the copolymers on the dispersion and distribution of nanoparticles in the matrix, as well as the synergy between the mixing components.

2. Materials and Methods

Tables 1 and 2 describe the materials used. The used block copolymer mass fraction was 20% and the nanoparticle mass fraction was 0.25%. The mixing method for the epoxy, epoxy/copolymer and nanocomposite/copolymer system was the same as that of Silva et al.[18]. The nanoparticles were dispersed in the block copolymer through mechanical stirring and high energy sonication and, then, the epoxy matrix was inserted and stirred for 10 minutes before the hardener was added. The mixture was poured into molds and cured at 60 °C for 24 h and post-cured at 100 °C for 1 h. Table 3 shows the adopted nomenclature.

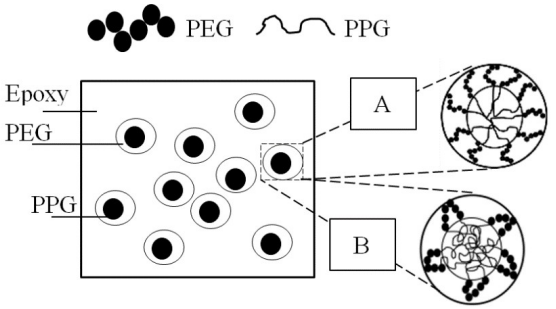

Figure 1. Schematic representation of the formation of micelle-type nanostructures when the PPG fraction is higher in the block copolymer: (A) PEG-b-PPG-b-PEG and (B) PPG-b-PEG-b-PPG.

The thermo-mechanical behavior was studied by means of dynamic-mechanical analysis (DMA) in a Q800 V21.1, Build 51, equipment. All samples were tested under single cantilever geometry (35.48x12.57x3.14mm^3) at 2 Hz, with the temperature in the range of 25 to 220 °C, using a heating rate of 3 °C/min in a synthetic atmosphere.

The morphological characteristics of the mixtures were investigated through field-based electron microscopy (SEM-FEG) using a JSM-6710F JEOL microscope and optical microscopy (TOM) on a U-TV05XC-3 OLYMPUS. For SEM-FEG were used criofracturated sample and for TOM the samples were cut to a nominal thickness of about 20 µm at room temperature in a PAT M LABORANA microtome.

The tensile test was performed on a universal testing machine, AM-5kN (Oswaldo Filizola), with a 5kN load cell and a test speed of 5 mm/min, at room temperature, according to ASTM D638[19]. The specimens were machined and sanded to comply with DIN 53504-S3A[20], with dimensions of 2x8.5x50 mm.

The Young's modulus was obtained by nanoindentation. Measurements were performed with nine nanoindentations arranged in a 3x3 matrix with a Berkovich-type tip. 9 cycles of 12 loadings and unloadings were used with variables of 0.2; 0.4; 0.78; 1.56; 3.13; 6.25; 12.5; 25; 50; 100; 200 and

Table 1. Physical properties of all materials used in this work, purchased from Sigma-Aldrich.

Material	Chemical Structure	Molar Mass (MM) (g mol^{-1})	Viscosity	PEG (wt%)
[1]DGEBA	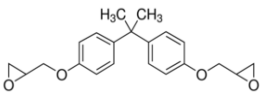	340.1	-	-
[2]DDM	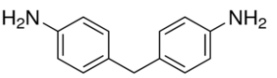	198.26	-	-
[3]PPG-b-PEG-b-PPG$_{50\%}$	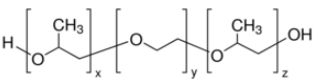	2000	480 cP (77°C, Brookiefield)	50
[4]PEG-b-PPG-b-PEG$_{30\%}$	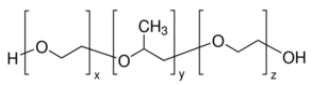	5800	350 cP (60°C, Brookiefield)	30

[1]Bisphenol A diglycidyl ether; [2]4,4 Diaminodiphenylmethanes; [3]Poly (propylene glycol) - block-poly (ethylene glycol) - block-poly (propylene glycol) with 50% PEG; [4]Poly (ethylene glycol) - block-poly (propylene glycol) - block-poly (ethylene glycol) with 30% PEG

Table 2. Characteristics of the nanoparticles.

Nanoparticles	ID	Geometry	Surface area (m^2/g)	Size	Supplier
[1] Carbon nanotube	CNT	Tubular	-	Ø140 nm Comp. 7 µm	*Strem Chemical*
Graphene	G	Platelets	120-150	Larg. 25 um Esp. 6-8 nm	*Strem Chemical*
Carbon Black	CB	Spherical shape	35	Ø64-74 nm	*Orion Enginered Carbons*

[1] Multi-walled Carbon Nanotubes.

400 m/N for a period of 15s each indentation, in which the maximum load was kept constant, always considering a Poisson Modulus of 0.4.

3. Results and Discussions

After curing, the samples with a block copolymer without the nanoparticles are transparent at room temperature, suggesting that there was no phase split during the curing process, which indicates miscibility. The miscibility is related to the fraction of PEG in the structure of the block copolymer[3], even though the copolymers are differently positioned if compared to the PEG (one at the ends and another in the center), showing that the copolymer architecture is not the predominant factor for the presented miscibility.

Figure 2 shows the transmission optical microscopy (TOM) images of the nanocomposites with and without block copolymers; the dark region is the nanoparticle clusters and the clear one is the epoxy/copolymer. No change was observed in the miscibility and dispersion of the block copolymers with the different morphologies and structures of the carbon nanoparticles used. However, the nanoparticles dispersion was influenced by their geometry, in addition to the contribution of the copolymer viscosity.

Table 3. Sample nomenclature.

Control		PPG- b- PEG- b- $PPG_{50\%}$	$PEG\text{-}b\text{-}PPG\text{-}b\text{-}PEG_{30\%}$
Neat Epoxy	P	P50	P30
Epoxy with 0,25% carbon nanotubes	PCNT	50CNT	30CNT
Epoxy with 0,25% graphene	PG	50G	30G
Epoxy with 0,25% carbon black	PCB	50CB	30CB

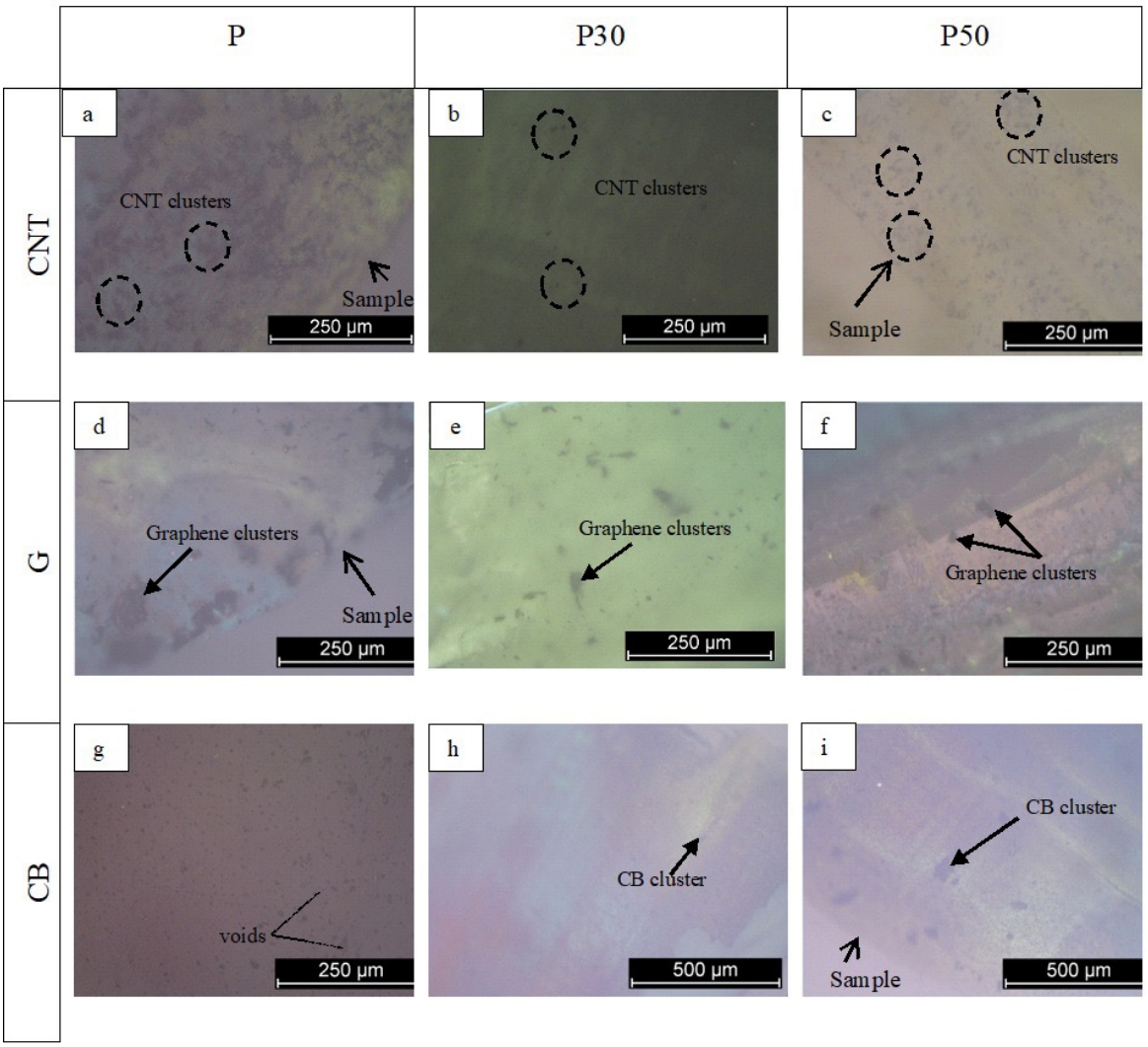

Figure 2. TOM Micrographs: (a) PCNT (b) 30CNT (c) 50CNT (d) PG (e) 30G (f) 50G (g) PCB (h) 30CB (i) 50CB. The dark region is the nanoparticle clusters and the clear one is the epoxy/copolymer.

The CNT dispersion into the epoxy is found with agglomerates in all samples, with and without a copolymer (Figure 2a, b and c). However, adding the block copolymer reduced the size of such agglomerates, both for nanocomposites with the PPG-b-PEG-b-$PPG_{50\%}$ copolymer and for PEG-b-PPG-b-$PEG_{30\%}$.

Nanocomposites with graphene without a copolymer, sample PG, presented a non-homogeneous distribution and dispersion, and their agglomerates are larger than those of CNTs, as shown in Figure 2d. The geometry of the graphene makes it difficult to disperse into the matrix, due to its planar surface area, making it more difficult to overcome Van der Waals interactions and to effectively separate each sheet[21]. When the copolymer is added, agglomerates are still observed, however smaller and better distributed in the epoxy (Figure 2e and Figure 2f). In general, the images show a trend of block copolymers reducing the size of the agglomerates and allowing a more homogeneous distribution of agglomerates. Similar results were also obtained by other authors with the use of block copolymer and graphene[22].

In the pure PCB nanocomposites (Figure 2g) and in 30CB with the PEG-b-PPG-b-$PEG_{30\%}$ copolymer (Figure 2h), no larger clusters were found, due to the presence of bubbles making smaller clusters difficult to identify. However, when the PPG-b-PEG-b-$PPG_{50\%}$ copolymer is added, 50CB system, particle agglomerates are found, as Figure 2-i shows, suggesting that this copolymer did not effectively contribute to the dispersion of the nanoparticles in the matrix.

Figure 3 presents the SEM-FEG images of the pure nanocomposites and of those with the block copolymers. Phase separation could not be visualized through microscopy, indicating that miscibility was obtained with this fraction of copolymer (20%), in agreement with previously published works[3,18].

Clusters of pure nanocomposite (PCNT) are in the size range of 42 ± 14 µm, whereas nanocomposites with the PEG-b-PPG-b-$PEG_{30\%}$ block copolymer (30CNT) are approximately 31.1 ± 10 µm, and those with PPG -b-PEG-b-$PPG_{50\%}$ (50CNT) are approximately 14.5 ± 8 µm, corroborating the optical microscopy results. These clusters were measured by ImageJ using the measured and averaged area of at least 10 clusters.

The CNT cluster region is indicated with rectangles and was measured with the ImageJ software. The images show CNT clusters in all samples, however both block copolymers contributed to a homogeneous distribution reduced their size.

The clusters for graphene nanocomposites can be found in the pure samples, and adding the copolymer altered their fracture surface. The agglomerates are indicated by black

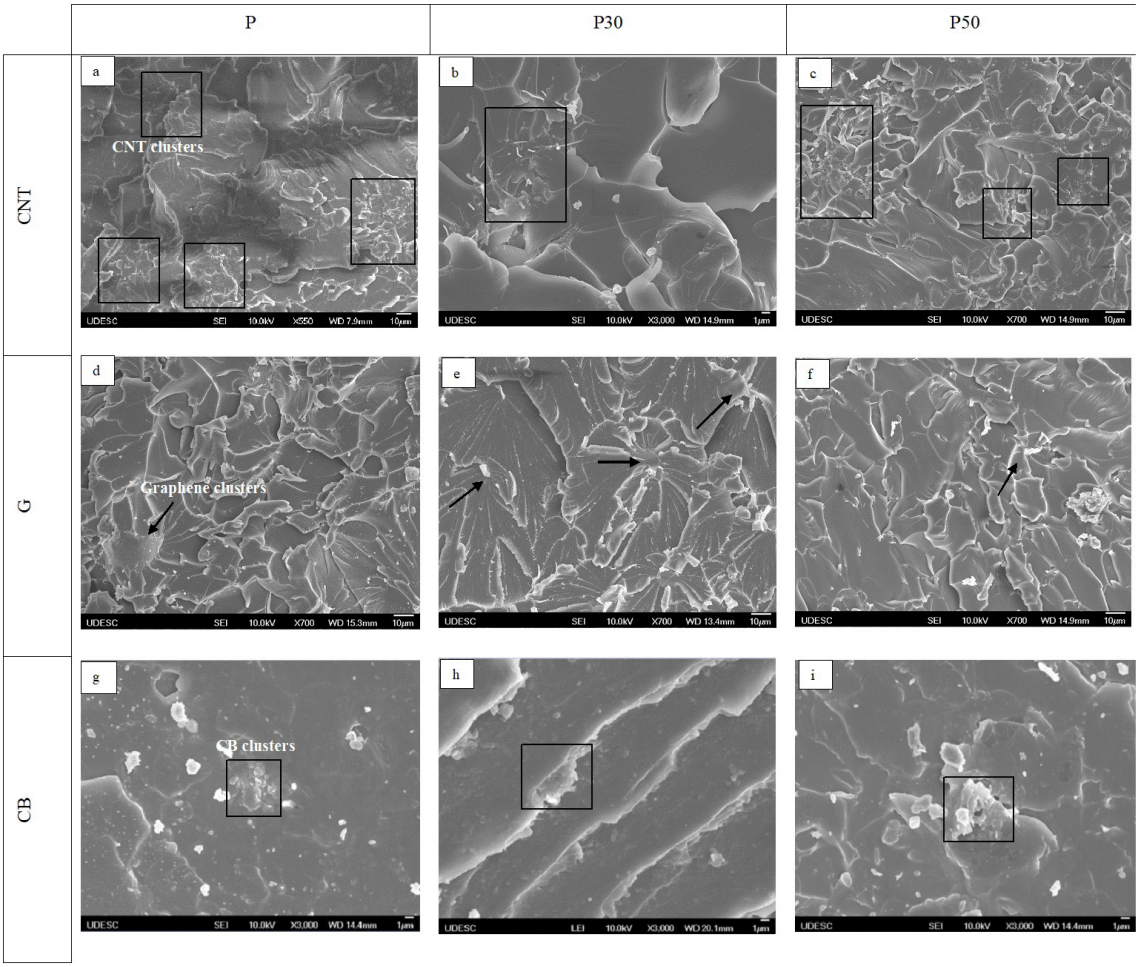

Figure 3. FEG micrographs: (a) PCNT (b) 30CNT (c) 50CNT (d) PG (e) 30G (f) 50G (g) PCB (h) 30CB (i) 50CB.

arrows. The PCB nanocomposite, on the other hand, based on what is seen in the literature[23], points to the region that is the possible location of the nanoparticles. As well as graphene, there is indication that the fracture surface was modified with the incorporation of copolymers, while, in the PCB sample, a fragile fracture surface can be verified, but not in the samples 50CB and 30CB. The results suggest that the viscosity may be interfering with the dispersion of the nanoparticles in the matrix: the PPG-b-PEG-b-$PPG_{50\%}$ copolymer has a higher viscosity than the PEG-b-PPG-b-$PEG_{30\%}$ (Table 1), which facilitates their dispersion. The well-known phenomenological Stokes-Einstein equation provides an explanation: the lower the viscosity, the higher the diffusion coefficient for a Brownian particle.

Figure 4 shows the dynamic mechanical response of all nanocomposites and Table 4 shows the values of T_g (glass transition temperature) and E' (storage modulus). The T_g of the epoxy decreased when the block copolymer (P50) was added, indicating miscibility or, at least, partial miscibility between the two components. Such reduction may result from the plasticization effect of the PEG chains, yielding a reduction in the crosslinking density of the epoxy network, which was also observed in other works[6,15,18,24]. Other authors[25-30] also observed the addition of soft particles slightly decreased the T_g of the matrix. The authors report these results reflect the smaller negative effect of the dispersed phase on the epoxy resin curing reaction.

Pure CNT nanocomposites (PCNT) showed a T_g reduction of approximately 30 °C. According to Costa et al.[31], adding reinforcements to the polymeric matrix can increase the number of microvoids, which can decrease T_g due to the presence of free volume. However, adding the copolymers to the nanocomposite caused an increase of approximately 46 °C for the 30CNT sample and 14 °C for 50CNT in relation to the pure nanocomposite (PCNT). Such difference

Table 4. Values of T_g, storage modulus (E'v) in the glass region (T = 30 ° C) and the storage modulus in the rubber region (E'b) (T = 75 ° C).

Samples	T_g (°C)	E'_v (GPa)	E'_b (GPa)	v (mol/mm^3)
P	142	1.80	0.064	8.39
P30	152	1.60	0.071	8.86
*P50	104	1.67	0.062	11.88
PCNT	111	2.05	0.088	103.24
30CNT	157	1.44	0.092	4.05
50CNT	125	1.77	0.046	165.63
PG	146	1.75	0.087	9.11
30G	151	1.67	0.075	9.39
50G	133	1.89	0.047	11.84
PCB	142	1.65	0.057	12.09
30CB	153	1.61	0.075	10.30
50CB	128	2.10	0.039	22.68

*Previously published values[18].

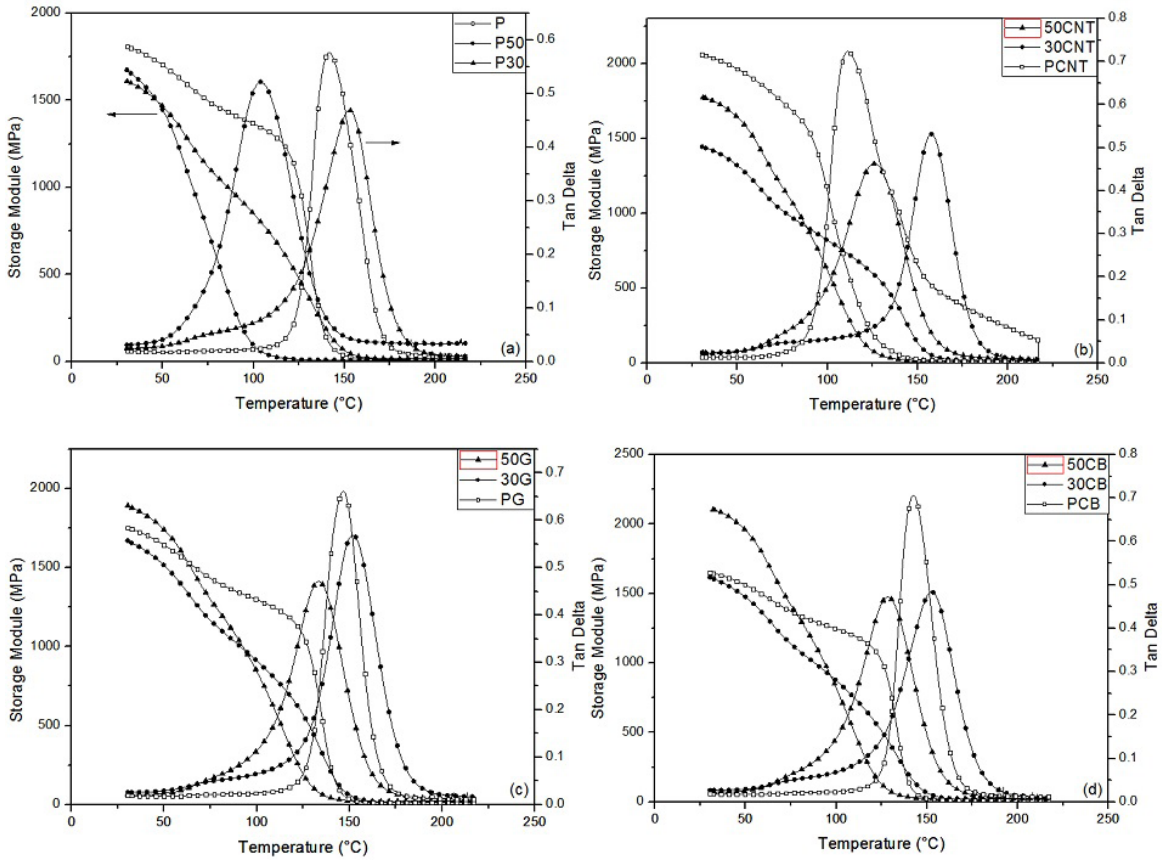

Figure 4. DMA curves: (a) Epoxy/copolymer, (b) PCNT nanocomposites, (c) PG nanocomposites and (d) PCB nanocomposites.

can be related to the diffusion factors, through which the block copolymers tend to decrease the resin viscosity and facilitate the dispersion of the nanoparticles, thus reducing the free volume caused by the microvoids formed by the nanoparticle agglomeration[16,32]. These results suggest that the block copolymers may be contributing to a better distribution and dispersion of the carbon nanotubes, corroborating the TOM and FEG images.

The DMA results also showed that the PEG-b-PPG-b-$PEG_{30\%}$ block copolymer contributed to an increase in T_g in the graphene nanocomposite (30G), both compared to the P (5 °C) and to the PG (9 °C). According to the literature[21], rigid nanoparticles can act as an obstacle to the molecular mobility of the resin. Therefore, these results suggest that the mobility near the interface/interphase has been altered. For the PPG-b-PEG-b-$PPG_{50\%}$ copolymer fraction, the nanoparticles did not inhibit the copolymer plasticization effect in the epoxy. Martin-Gallego et al.[24] obtained different results in their research, attributing the T_g change in graphene nanocomposites to a strong matrix-nanoparticle interface, in a way that the functionalized graphene produced a greater T_g increase.

For carbon black nanocomposites (PCB), there is no significant change in T_g if compared to pure epoxy. However, as observed in graphene and CNT, samples with the block copolymer with the lowest PEG fraction (30%) resulted in the highest T_g, such as an increase of 11 °C in relation to the pure nanocomposite, while nanocomposites with the 50% PEG copolymer showed a T_g reduction of approximately 14 °C. According to Costa et al.[31], the addition of polymer matrix reinforcements can increase the amount of microvoids, the presence of these microvoids can cause a decrease in T_g due to the presence of free volume, as observed in the TOM images. The same was reported by Silva et al.[33].

This increase in T_g after adding the nanoparticles may have occurred due to their dispersion in the matrix. The micrographs (Figures 2 and 3) show that the PEG-b-PPG-b-$PEG_{30\%}$ had smaller clusters and a more even effective distribution than the PPG-b-PEG-b-$PPG_{50\%}$. Jayan et al.[15] used the same block copolymer, PEG-b-PPG-b-$PEG_{30\%}$, to disperse graphene oxide in epoxy, and reported that the increase in T_g is due to the confinement of epoxy chains on the surface of the nanoparticles, which reduces the chain mobility, functioning as a physical interlock, and that the nanoparticle clusters can negatively affect this confinement, causing the reduction of T_g.

The scheme in Figure 5 shows an interfacial layer formation at the nanoparticle interface due to the cured adsorbed epoxy. According to the micrographs (Figure 2), there is an indication that the interface quality between particle and matrix is improved after the block copolymers incorporation , which is consistent with the Tg results, and similar results to the works[25,34,35].Thus, the presence of the PEG-b-PPG-b-$PEG_{30\%}$ block copolymer facilitates the crosslinking between the epoxy chains, hindering mobility at the interface, yielding higher T_g values[16,32]. As reported by Pascault et al.[5], the PEG block allows a greater molecular mobility in the chain, due to its physical interactions with the epoxy-crosslinked aromatic amine, so the results suggest that the largest fraction of PPG (70%) in the copolymer structure acted for such interlocking effect. Even though the PEG is at the end of the chain, its percentage at the ends (20%) is lower than its total[36], suggesting that the PPG hindered the mobility of the epoxy at the interface, resulting in higher values of T_g. The nanocomposites with PPG-b-PEG-b-$PPG_{50\%}$, on the other hand, presented a higher fraction of PEG (50%), resulting in greater molecular mobility, which hinders the interlocking effect, yielding lower T_g values than that of nanocomposites with PEG- b-PPG-b-$PEG_{30\%}$.

Comparing the values of E' shows that, for the PCNT, stiffness was obtained in the glassy and rubbery regions with a 14% and 38% increase, respectively, in the storage modulus in relation to the epoxy. When the block copolymer is added in relation to the pure nanocomposite, there is a 14% drop for the 50CNT sample and 30% for the 30CNT for the

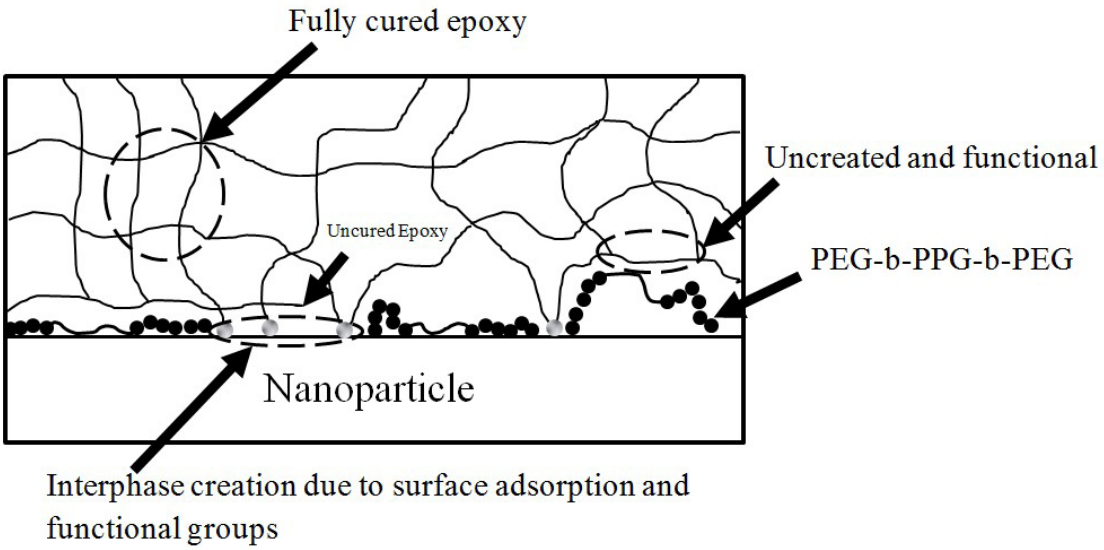

Figure 5. Schematic representation of the physical interlocking of epoxy nanocomposites with PEG-b-PPG-b-$PEG_{30\%}$ block copolymer. Adapted from Kulkarni et al.[16].

glassy regions; and for the rubbery regions there is a 48% drop for the 50CNT sample and a slightly increased (5%) for the 30CNT. This drop may be related to the molecular mobility of PPG in the epoxy. However, comparing these results in the glassy regions with the samples without nanoparticles (with copolymers only) shows a decrease of approximately 10% for the 30CNT sample in relation to the P30 sample, and a 6% increase in E' for the 50NTC sample in relation to the P50 sample. Thus, the results suggest that the copolymer with the highest fraction (50%) of PEG in its structure contributes to a synergistic effect between the CNT nanoparticles and the matrix, where an increase in E' is observed. Jyoti et al.[37] showed that the increase in the storage modulus is related to the increase in interfacial adhesion. The dispersion of both nanoparticles may be related to the surface area, which differs with the different geometries used in this work. These results suggest that the adhesion between NTC and matrix was increased with the incorporation of block copolymers.

In relation to the pure graphene nanocomposite (PG), the 30G sample obtained a 5% reduction in E'_v, in contrast to the 50G sample, which obtained an increase of 8%. And, for carbon black nanocomposites, the PEG-b-PPG-b-$PEG_{30\%}$ block copolymer did not cause any significant changes in E'_v, however an increase of approximately 27% was observed for the 50CB sample in relation to the pure nanocomposite. These results suggest that the plasticization effect of the PPG-b-PEG-b-$PPG_{50\%}$ block copolymer can be inhibited by the incorporation of graphene nanoparticles, which was not observed for the PEG-b-PPG-b-$PEG_{30\%}$ block copolymer. It should be kept in mind that the copolymer with PEG 30% is less viscous than the copolymer with 50%.

The effectiveness of nanoparticles in terms of mechanical behavior can be measured through factor C, from Equation 1, where E'_v is the storage modulus in the glass region and E'_b is the storage modulus in the rubber region. Figure 6 shows these values obtained for all studied nanocomposites.

$$C = \frac{\frac{E'_v}{E'_b}composites}{\frac{E'_v}{E'_b}pure} \quad (1)$$

From the results of the storage modulus (E'), the degree of entanglement (N), Equation 2, which is an indirect measure of nanoparticle dispersion in the matrix, can be calculated. The higher the N, the weaker the interactions between the nanoparticle and the matrix, resulting in a less effective dispersion[37].

$$N = \frac{E'}{6RT} \quad (2)$$

Where 'N' is the degree of entanglement, E' is the storage modulus in absolute temperature, R is the ideal gas constant and T is the absolute temperature (K).

The factor 'C' indicates the effective contribution of nanoparticles in this transition process from the vitreous to the rubbery state, and the lower its value, the more effective the action of the nanoparticles[38]. The results, Figure 6a, show that the efficiency of the nanoparticles in the matrix depended on the incorporation of the type of block copolymer added to the nanocomposite. The 'C' values of the nanocomposites with PEG-b-PPG-b -$PEG_{30\%}$ were very close to those of the pure nanocomposites, and the nanocomposites with PPG-b-PEG-b-$PPG_{50\%}$ already presented high values. These results agree with E': the effect of the nanoparticles overlaps the plasticization effect.

The results of the 'N' Factor, Figure 6b, confirm that the copolymer with 30% PEG contributed to a more effective nanoparticle dispersion, corroborating the microscopy images. The carbon black showed a higher value of 'N' compared to other nanocomposites with the PPG-b-PEG-b-$PPG_{50\%}$, suggesting that the copolymer did not contribute to the effective dispersion of the nanoparticles, which was reflected on the values of E'_v and can be justified by the size of the nanoparticle clusters in the matrix. Another factor to observe is that the copolymer helped the interaction between the nanoparticles and the matrix, as suggested by the results of the 'N' factor, and that such interaction is influenced by the geometry of the nanoparticle, presenting higher 'N' values for graphene.

The DMA results also allow the calculation of the crosslink density (ν) given by Equation 3[39,40]:

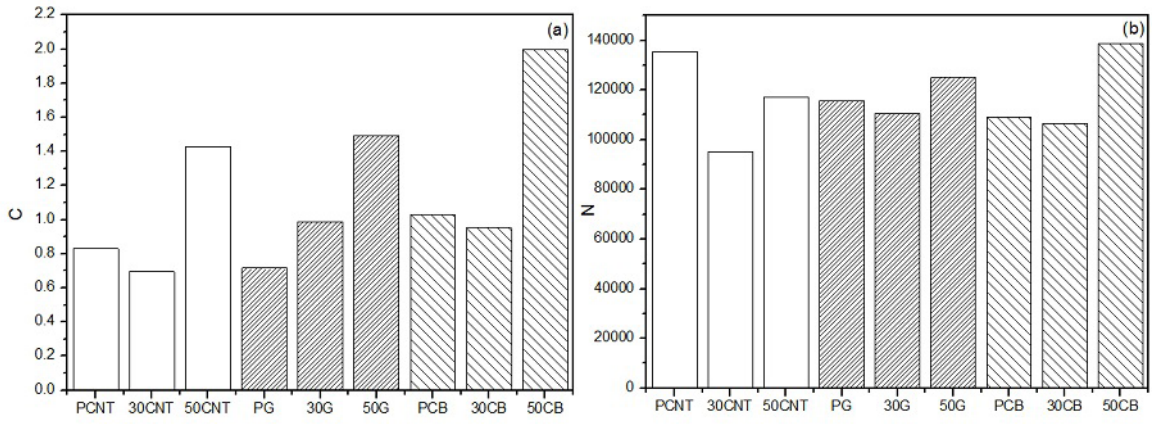

Figure 6. Values of factors C (a) and N (b) for nanocomposites with and without a block copolymer.

$$v = \frac{E_r}{3RT_r} \quad (3)$$

Where T_r is the temperature above T_g, Er is the storage modulus corresponding to Tr obtained from DMA data and R is the real gas constant. The results of crosslink density (v), Table 4, show that it was reduced after the incorporation of the PEG-b-PPG-b-$PEG_{30\%}$ block copolymer and that can be explained by the restricted mobility at the interface due to the interactions between the epoxy and the nanoparticles, as the nanoparticles interrupt the crosslink network. These results are in line with the work of Jayan et al.[15].

Figure 7 shows the Young's modulus results obtained from nanoindentation measurements and de ultimate stress from the tensile test. The storage modulus (E') behavior at room temperature is similar to the Young's modulus: the highest E' for the pure epoxy (P), decreasing as copolymers are added, 27% for PEG-b-PPG-b-$PEG_{30\%}$ and 7% for PPG-b-PEG-b-$PPG_{50\%}$, according to Figure 7-a, which was expected with the incorporation of a soft phase in a thermoset matrix. Larrañaga et al.[41] and Dean et al.[42] also obtained a reduction in the modulus with the incorporation of a block copolymer in the matrix, the authors justify that this decrease in the storage module is due to the PEO:PPO ratio. The PEG fractions are higher for the PPG-b-PEG-b-PPG50% copolymer, it is assumed that the interactions between this PEG block and the epoxy matrix are more likely for the P50 sample, thus explaining this behavior.

Pure nanocomposites had a drop in E when compared to pure epoxy (P): 18% for graphene (PG), 11% for CNT (PCNT) and carbon black (PCB) nanoparticles. However, the incorporation of carbon nanoparticles inhibited the plasticizer effect of the PPG-b-PEG-b-$PPG_{50\%}$ copolymer. There are 20% increases in E in all systems in relation to pure nanocomposites, corroborating the behavior observed through DMA, which may be related to the presence of agglomerates in the matrix, even with the incorporation of block copolymers[22]. These results suggest that the PPG-b-PEG-b-$PPG_{50\%}$ copolymer contributed to the synergistic effect between the nanoparticles and the matrix, and may also have minimized the plasticization effect of the block copolymer. Martin-Gallego et al.[24] obtained similar results, in which nanoparticles inhibited the plasticization effect of the block copolymer in the matrix, hindering the molecular mobility.

The geometry of the nanoparticles may be interfering with the mechanical properties, as reported in the DMA results. Carbon black nanocomposites showed significant increases in E values, being 22% for both copolymers. The spherical surface may be contributing to a greater synergy between the nanoparticles and the matrix, that is, the smaller the interface, the greater the contribution of the block copolymer. Another hypothesis would be that the difference in E is related to the dispersion of the nanoparticles into the matrix[18,24], as it was observed through microscopy that the block copolymer with the lowest PEG fraction provided a more effective dispersion and distribution of the nanoparticles, while the copolymer with 50% shows greater evidence of agglomerates, however with better mechanical results.

The interface between particles and the surrounding polymer matrix and their characteristics strongly impacts the properties of nanocomposites[16,32], as seen in Figure 4. One of the factors that may interfere with the effect of nanoparticles on mechanical properties would be their number, which depends on their volume and their volume fraction in the nanocomposite. Assuming the same volume fraction, the number of spherical particles is significantly higher than tube or platelet-shaped nanoparticles. As a result, a greater number of reinforcements could provide a stronger stiffening effect that occurs through the interaction between the reinforcement phase and the original material. This trend corroborates the traction results shown in Figure 7, where the carbon black nanocomposites showed a greater Young's modulus. Alishahi et al.[43] studied theoretical models to analyze the interference of carbon nanoparticle geometry in the properties of epoxy nanocomposites. According to the interface volume per unit of particle volume, spherical nanoparticles are more likely to improve the properties of nanocomposites compared to tubes or platelets, while offering greater interface volume, which can further enhance such properties. However, if carbon nanotubes are compared to graphene, the theoretical models show that nanotubes lead to better mechanical properties than platelets.

The tensile strength (σ_r) is another indication of adhesion between matrix and particles. Increases in σ_r indicate adhesion between matrix and reinforcement[44]. The DMA

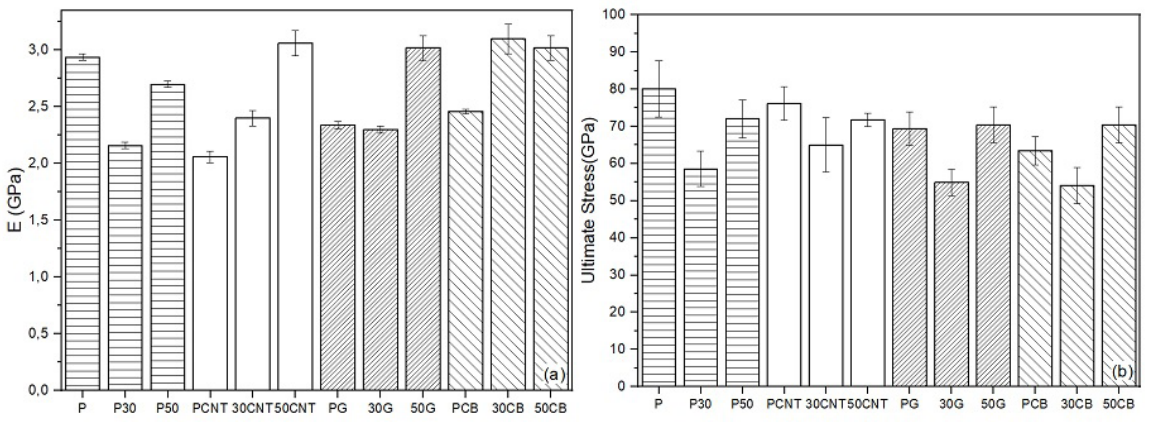

Figure 7. Results of mechanical properties: (a) Young's modulus and (b) Ultimate stress.

results show that Tg was higher for nanocomposites with the PEG-b-PPG-b-$PEG_{30\%}$ block copolymer, but E' and E were lower. According to Figure 7b, for all nanoparticles, there is a reduction in rupture stress of approximately 15%. Thus, the results suggest that, although this copolymer contributes to the distribution of the nanoparticles and inhibits the plasticizer effect in the matrix, according to the Tg results, it may not be helping the nanoparticle-matrix adhesion. The opposite is observed for the PPG-b-PEG-b-$PPG_{50\%}$ block copolymer, in which there is nanoparticle-matrix synergy as the copolymer is incorporated, with increases of up to 15% in the rupture stress. Therefore, this block copolymer may be more effective regarding the mechanical properties of these nanocomposites, indicating that higher fractions of PEG in the resin may result in greater interaction capacity between them, while contributing to a greater adhesion between the nanoparticle and the matrix, yielding the previously reported mechanical results.

The results also suggest that, after the occurrence of stress concentrations, the CB nanoparticles absorb more energy, due to an increased free volume of the material, which participates in this deformation process. In addition, graphene has an additional layer separation fracture mode. Due to their creased structure, the layers are capable of mechanically interlocking and, therefore, are more likely to separate under transversal stress than under shear loads[45]. Therefore, depending on the orientation of the graphene particles, particle separation or detachment from the matrix may occur[22,46,47]. Both mechanisms are accompanied by plastic deformation of the surrounding matrix.

4. Conclusion

The advance of this work in relation to the current literature would be that the results suggest that the miscibility of the triblock copolymer with PEG/PPG blocks is influenced by the proportion of PEG in the block copolymer, regardless of its position in the copolymer structure. Regarding nanocomposites, it was observed that the dispersion is related to the higher viscosity of the copolymer, that viscosities contribute to a better dispersion/distribution of the nanoparticles in the matrix.

The copolymer with the 30% PEG fraction, on the other hand, contributed to the dispersion and distribution of the nanoparticles in the epoxy matrix, increasing the T_g of the nanocomposites in relation to the epoxy/copolymer system. However, the mechanical results of these nanocomposites were inferior when compared to the others. The results suggest that the copolymer viscosity may have contributed to the distribution of the nanoparticle clusters, and the physical interactions of the PEG block (50%) with the epoxy-crosslinked aromatic amine contributed to an improvement in mechanical properties. Thus, both copolymers contributed significantly to the properties of the nanocomposites, one towards the dispersion and distribution of the nanoparticles, yielding higher T_g values, and the other contributed to the mechanical properties of the nanocomposites.

5. Acknowledgments

This study was partially financed by the Coordenação de Aperfeicoamento de Pessoal de Nivel Superior - Brasil (CAPES) - Finance Code 001. The authors would like to thank CNPq and FAPESC/PAP for the financial resources.

6. References

1. George SM, Puglia D, Kenny JM, Causin V, Parameswaranpillai J, Thomas S. Morphological and mechanical characterization of nanostructured thermosets from epoxy and styrene-*block*-butadiene-*block*-styrene triblock copolymer. Ind Eng Chem Res. 2013;52(26):9121-9. http://dx.doi.org/10.1021/ie400813v.
2. Pandit R, Berkessel A, Lach R, Grellmann W, Adhikari R. Synthesis and characterization of nanostructured blends of epoxy resin and block copolymers. Nepal J Sci Technol. 2012;13(1):81-8. http://dx.doi.org/10.3126/njst.v13i1.7445.
3. Silva BL, Bello RH, Coelho LAF. The role of the ratio (PEG:PPG) of a triblock copolymer (PPG-b-PEG-b-PPG) in the cure kinetics, miscibility and thermal and mechanical properties in an epoxy matrix. Polym Int. 2018;67(9):1248-55. http://dx.doi.org/10.1002/pi.5633.
4. Wang T, Wang J, Chen W, Duan H, Xiao H, Wang J, et al. Toughening epoxy resins by modification with in situ polymerized acrylate copolymer composed of butyl acrylate and glycidyl methacrylate. High Perform Polym. 2015;27(2):177-82. http://dx.doi.org/10.1177/0954008314542473.
5. Pascault J-P, Williams RJJ. Epoxy polymers: new materials and innovations. 1st ed. Weinheim: Wiley-VCH; 2010. General concepts about epoxy polymers.
6. Larrañaga M, Martín MD, Gabilondo N, Kortaberria G, Corcuera MA, Riccardi CC, et al. Cure kinetics of epoxy systems modified with block copolymers. Polym Int. 2004;53(10):1495-502. http://dx.doi.org/10.1002/pi.1574.
7. Hillmyer MA, Lipic PM, Hajduk DA, Almdal K, Bates FS. Self-assembly and polymerization of epoxy resin-amphiphilic block copolymer nanocomposites. J Am Chem Soc. 1997;119(11):2749-50. http://dx.doi.org/10.1021/ja963622m.
8. Guo Q, Thomann R, Gronski W, Thurn-Albrecht T. Phase behavior, crystallization, and hierarchical nanostructures in self-organized thermoset blends of epoxy resin and amphiphilic poly(ethylene oxide)-block-poly(propylene oxide)-block-poly(ethylene oxide) triblock copolymers. Macromolecules. 2002;35(8):3133-44. http://dx.doi.org/10.1021/ma011971h.
9. Mijovic J, Shen M, Sy JW, Mondragon I. Dynamics and morphology in nanostructured thermoset network/block copolymer blends during network formation. Macromolecules. 2000;33(14):5235-44. http://dx.doi.org/10.1021/ma991894e.
10. Ritzenthaler S, Court F, Girard-Reydet E, Leibler L, Pascault JP. ABC Triblock copolymers/epoxy-diamine blends. 2. Parameters controlling the morphologies and properties. Macromolecules. 2003;36(1):118-26. http://dx.doi.org/10.1021/ma0211075.
11. Tanaka T. Dielectric nanocomposites with insulating properties. IEEE Trans Dielectr Electr Insul. 2005;12(5):914-28. http://dx.doi.org/10.1109/TDEI.2005.1522186.
12. Serrano E, Martin MD, Tercjak A, Pomposo JA, Mecerreyes D, Mondragon I. Nanostructured thermosetting systems from epoxidized styrene butadiene block copolymers. Macromol Rapid Commun. 2005;26(12):982-5. http://dx.doi.org/10.1002/marc.200500131.
13. Dean JM, Verghese NE, Pham HQ, Bates FS. Nanostructure toughened epoxy resins. Macromolecules. 2003;36(25):9267-70. http://dx.doi.org/10.1021/ma034807y.
14. Jayan JS, Saritha A, Joseph K. Innovative materials of this era for toughening the epoxy matrix: A review. Polym Compos. 2018;39(S4):E1959-86. http://dx.doi.org/10.1002/pc.24789.
15. Jayan JS, Saritha A, Deeraj BDS, Joseph K. Triblock copolymer grafted Graphene oxide as nanofiller for toughening of epoxy resin. Mater Chem Phys. 2020;248:122930. http://dx.doi.org/10.1016/j.matchemphys.2020.122930.
16. Kulkarni HB, Tambe PB, Joshi GM. Influence of surfactant assisted exfoliation of hexagonal boron nitride nanosheets on mechanical, thermal and dielectric properties of epoxy

Nanocomposites. Compos Interfaces. 2020;27(6):529-50. http://dx.doi.org/10.1080/09276440.2019.1663115.
17. Gao J, Li J, Zhao S, Benicewicz BC, Hillborg H, Schadler LS. Effect of graft density and molecular weight on mechanical properties of rubbery block copolymer grafted SiO2 nanoparticle toughened epoxy. Polymer. 2013;54(15):3961-73. http://dx.doi.org/10.1016/j.polymer.2013.05.033.
18. Silva BL, Schuster MB, Bello R, Becker D, Coelho LA. The role of carbon nanoparticles in epoxy-based nanocomposites modified with (poly[polypropylene oxide]-block-poly[ethylene oxide]-block-poly[propylene oxide]) triblock copolymers on phase morphology and mechanical properties. Polym Compos. 2020;41(10):4243-52. http://dx.doi.org/10.1002/pc.25707.
19. ASTM: American Society for Testing and Materials. ASTM D638: standard test method for tensile properties of plastics. West Conshohocken: ASTM International; 2014.
20. DIN: Deutsches Institut fur Normung. DIN 53504 S3A: testing of rubber: determination of tensile strength at break, tensile stress at yield, elongation at break and stress values in a tensile test. Berlin: DIN; 2017.
21. Chakraborty AK, Plyhm T, Barbezat M, Necola A, Terrasi GP. Carbon nanotube (CNT)–epoxy nanocomposites: a systematic investigation of CNT dispersion. J Nanopart Res. 2011;13(12):6493-506. http://dx.doi.org/10.1007/s11051-011-0552-3.
22. Schuster MB, Opelt CV, Becker D, Coelho LAF. Role and sinergy of block copolymer and carbon nanoparticles on toughness in epoxy matrix. Polym Compos. 2018;39(S4):E2262-73. http://dx.doi.org/10.1002/pc.24599.
23. Li J, Wong P-S, Kim J-K. Hybrid nanocomposites containing carbon nanotubes and graphite nanoplatelets. Mater Sci Eng A. 2008;483–484:660-3. http://dx.doi.org/10.1016/j.msea.2006.08.145.
24. Martin-Gallego M, Verdejo R, Gestos A, Lopez-Manchado MA, Guo Q. Morphology and mechanical properties of nanostructured thermoset/block copolymer blends with carbon nanoparticles. Compos Part Appl Sci Manuf. 2015;71:136-43. http://dx.doi.org/10.1016/j.compositesa.2015.01.010.
25. Guan L-Z, Wan Y-J, Gong L-X, Yan D, Tang L-C, Wu L-B, et al. Toward effective and tunable interphases in graphene oxide/epoxy composites by grafting different chain lengths of polyetheramine onto graphene oxide. J Mater Chem A Mater Energy Sustain. 2014;2(36):15058-69. http://dx.doi.org/10.1039/C4TA02429J.
26. Gong L-X, Zhao L, Tang L-C, Liu H-Y, Mai Y-W. Balanced electrical, thermal and mechanical properties of epoxy composites filled with chemically reduced graphene oxide and rubber nanoparticles. Compos Sci Technol. 2015;121:104-14. http://dx.doi.org/10.1016/j.compscitech.2015.10.023.
27. Tang L-C, Zhang H, Sprenger S, Ye L, Zhang Z. Fracture mechanisms of epoxy-based ternary composites filled with rigid-soft particles. Compos Sci Technol. 2012;72(5):558-65. http://dx.doi.org/10.1016/j.compscitech.2011.12.015.
28. Tang L-C, Wan Y-J, Peng K, Pei Y-B, Wu L-B, Chen L-M, et al. Fracture toughness and electrical conductivity of epoxy composites filled with carbon nanotubes and spherical particles. Compos Part A. 2013;45:95-101. http://dx.doi.org/10.1016/j.compositesa.2012.09.012.
29. Tang L-C, Wan Y-J, Yan D, Pei Y-B, Zhao L, Li Y-B, et al. The effect of graphene dispersion on the mechanical properties of graphene/epoxy composites. Carbon. 2013;60:16-27. http://dx.doi.org/10.1016/j.carbon.2013.03.050.
30. Tang L-C, Wang X, Wan Y-J, Wu L-B, Jiang J-X, Lai G-Q. Mechanical properties and fracture behaviors of epoxy composites with multi-scale rubber particles. Mater Chem Phys. 2013;141(1):333-42. http://dx.doi.org/10.1016/j.matchemphys.2013.05.018.
31. Costa ML, Paiva JMF, Botelho EC, Rezende MC. Avaliação térmica e reológica do ciclo de cura do pré-impregnado de carbono/epóxi. Polímeros. 2003;13(3):188-97. http://dx.doi.org/10.1590/S0104-14282003000300009.
32. Szymoniak P, Pauw BR, Qu X, Schönhals A. Competition of nanoparticle-induced mobilization and immobilization effects on segmental dynamics of an epoxy-based nanocomposite. Soft Matter. 2020;16(23):5406-21. http://dx.doi.org/10.1039/D0SM00744G.
33. Silva DD, Silva DD, dos Santos WF, Pezzin SH. Nanocompósitos de matriz epoxídica com reforços produzidos a partir do grafite natural. Rev Mat. 2013;18:1216-72.
34. Gong L-X, Pei Y-B, Han Q-Y, Zhao L, Wu L-B, Jiang J-X, et al. Polymer grafted reduced graphene oxide sheets for improving stress transfer in polymer composites. Compos Sci Technol. 2016;134:144-52. http://dx.doi.org/10.1016/j.compscitech.2016.08.014.
35. Wan Y-J, Tang L-C, Gong L-X, Yan D, Li Y-B, Wu L-B, et al. Grafting of epoxy chains onto graphene oxide for epoxy composites with improved mechanical and thermal properties. Carbon. 2014;69:467-80. http://dx.doi.org/10.1016/j.carbon.2013.12.050.
36. Sigma-Aldrich. Data sheet: poly(ethylene glycol)-block-poly(propylene glycol)-block-poly(ethylene glycol). St. Louis.
37. Jyoti J, Singh BP, Arya AK, Dhakate SR. Dynamic mechanical properties of multiwall carbon nanotube reinforced ABS composites and their correlation with entanglement density, adhesion, reinforcement and C factor. RSC Advances. 2016;6(5):3997-4006. http://dx.doi.org/10.1039/C5RA25561A.
38. Hameed N, Sreekumar PA, Francis B, Yang W, Thomas S. Morphology, dynamic mechanical and thermal studies on poly(styrene-co-acrylonitrile) modified epoxy resin/glass fibre composites. Compos Part Appl Sci Manuf. 2007;38(12):2422-32. http://dx.doi.org/10.1016/j.compositesa.2007.08.009.
39. Lee C-H, Park J-J. The properties of DMA and DSC for epoxy nanoand-micro mixture composites. Trans Electr Electron Mater. 2010;11(2):69-72. https://doi.org/10.4313/TEEM.2010.11.2.069.
40. Souza JPB, Reis JML. A thermomechanical and adhesion analysis of epoxy/Al2O3 nanocomposites. Nanomater Nanotechnol. 2015;5(18):1-7. https://doi.org/10.5772/60938.
41. Larrañaga M, Serrano E, Martin MD, Tercjak A, Kortaberria G, de la Caba K, et al. Mechanical properties–morphology relationships in nano-/microstructured epoxy matrices modified with PEO–PPO–PEO block copolymers. Polym Int. 2007;56(11):1392-403. http://dx.doi.org/10.1002/pi.2289.
42. Dean JM, Lipic PM, Grubbs RB, Cook RF, Bates FS. Micellar structure and mechanical properties of block copolymer-modified epoxies. J Polym Sci, B, Polym Phys. 2001;39(23):2996-3010. http://dx.doi.org/10.1002/polb.10062.
43. Alishahi E, Shadlou S, Doagou-R S, Ayatollahi MR. Effects of carbon nanoreinforcements of different shapes on the mechanical properties of epoxy-based nanocomposites. Macromol Mater Eng. 2013;298(6):670-8. http://dx.doi.org/10.1002/mame.201200123.
44. Karihaloo B, Huang X. Tensile response of quasi-brittle materials. Pure Appl Geophys. 1991;137(4):461-87. http://dx.doi.org/10.1007/BF00879045.
45. Knoll JB, Riecken BT, Kosmann N, Chandrasekaran S, Schulte K, Fiedler B. effect of carbon nanoparticles on the fatigue performance of carbon fibre reinforced epoxy. Compos Part A. 2014;67:233-40. http://dx.doi.org/10.1016/j.compositesa.2014.08.022.
46. Schuster MB, Coelho LAF. Toughness and roughness in hybrid nanocomposites of an epoxy matrix. Polym Eng Sci. 2019;59(6):1258-69. http://dx.doi.org/10.1002/pen.25109.
47. Chandrasekaran S, Sato N, Tolle F, Mülhaupt R, Fiedler B, Schulte K. Fracture toughness and failure mechanism of graphene based epoxy composites. Compos Sci Technol. 2014;97:90-9. http://dx.doi.org/10.1016/j.compscitech.2014.03.014.